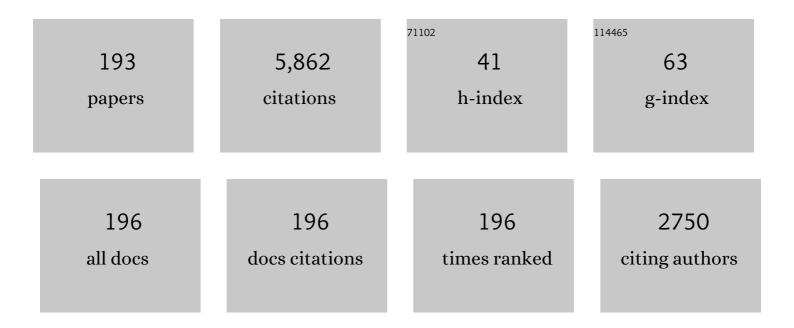


List of Publications by Year in descending order

Source: https://exaly.com/author-pdf/6799324/publications.pdf Version: 2024-02-01



#	Article	IF	CITATIONS
1	Qualitative and quantitative ultrashort echo time (UTE) imaging of cortical bone. Journal of Magnetic Resonance, 2010, 207, 304-311.	2.1	204
2	UTE imaging in the musculoskeletal system. Journal of Magnetic Resonance Imaging, 2015, 41, 870-883.	3.4	197
3	Quantitative ultrashort echo time (UTE) MRI of human cortical bone: Correlation with porosity and biomechanical properties. Journal of Bone and Mineral Research, 2012, 27, 848-857.	2.8	148
4	Short T2 contrast with three-dimensional ultrashort echo time imaging. Magnetic Resonance Imaging, 2011, 29, 470-482.	1.8	128
5	Qualitative and quantitative ultrashortâ€TE MRI of cortical bone. NMR in Biomedicine, 2013, 26, 489-506.	2.8	125
6	Ultrashort echo time imaging with bicomponent analysis. Magnetic Resonance in Medicine, 2012, 67, 645-649.	3.0	119
7	Ultrashort echo time (UTE) imaging with bi-component analysis: Bound and free water evaluation of bovine cortical bone subject to sequential drying. Bone, 2012, 50, 749-755.	2.9	106
8	Ultrashort echo time spectroscopic imaging (UTESI): an efficient method for quantifying bound and free water. NMR in Biomedicine, 2012, 25, 161-168.	2.8	102
9	Ultrashort Echo Time MR Imaging of Osteochondral Junction of the Knee at 3 T: Identification of Anatomic Structures Contributing to Signal Intensity. Radiology, 2010, 254, 837-845.	7.3	98
10	UTE imaging with simultaneous water and fat signal suppression using a time-efficient multispoke inversion recovery pulse sequence. Magnetic Resonance in Medicine, 2016, 76, 577-582.	3.0	91
11	Dual inversion recovery, ultrashort echo time (DIR UTE) imaging: Creating high contrast for shortâ€ <i>T</i> ₂ species. Magnetic Resonance in Medicine, 2010, 63, 447-455.	3.0	89
12	Ultrashort TE <i>T</i> ₁ rho (UTE <i>T</i> ₁ rho) imaging of the Achilles tendon and meniscus. Magnetic Resonance in Medicine, 2010, 64, 834-842.	3.0	88
13	Ultrashort echo time (UTE) magnetic resonance imaging of the short T2 components in white matter of the brain using a clinical 3T scanner. NeuroImage, 2014, 87, 32-41.	4.2	88
14	Ultrashort echo time spectroscopic imaging (UTESI) of cortical bone. Magnetic Resonance in Medicine, 2007, 58, 1001-1009.	3.0	85
15	Ultrashort TE spectroscopic imaging (UTESI): Application to the imaging of short T2 relaxation tissues in the musculoskeletal system. Journal of Magnetic Resonance Imaging, 2009, 29, 412-421.	3.4	83
16	Quantitative Characterization of the Achilles Tendon in Cadaveric Specimens: T1 and T2 [*] Measurements Using Ultrashort-TE MRI at 3 T. American Journal of Roentgenology, 2009, 192, W117-W124.	2.2	76
17	Magic angle effect in magnetic resonance imaging of the Achilles tendon and enthesis. Magnetic Resonance Imaging, 2009, 27, 557-564.	1.8	73
18	Bone cell-independent benefits of raloxifene on the skeleton: A novel mechanism for improving bone material properties. Bone, 2014, 61, 191-200.	2.9	72

#	Article	IF	CITATIONS
19	Ultrashort–Echo Time MR Imaging of the Patella with Bicomponent Analysis: Correlation with Histopathologic and Polarized Light Microscopic Findings. Radiology, 2012, 264, 484-493.	7.3	69
20	Accurate T ₁ mapping of short T ₂ tissues using a threeâ€dimensional ultrashort echo time cones actual flip angle imagingâ€variable repetition time (3D UTEâ€Cones AFIâ€VTR) method. Magnetic Resonance in Medicine, 2018, 80, 598-608.	3.0	69
21	Quantitative magnetization transfer ultrashort echo time imaging using a timeâ€efficient 3D multispoke Cones sequence. Magnetic Resonance in Medicine, 2018, 79, 692-700.	3.0	68
22	Two-dimensional ultrashort echo time imaging using a spiral trajectory. Magnetic Resonance Imaging, 2008, 26, 304-312.	1.8	66
23	Assessment of cortical bone with clinical and ultrashort echo time sequences. Magnetic Resonance in Medicine, 2013, 70, 697-704.	3.0	66
24	Self-attention convolutional neural network for improved MR image reconstruction. Information Sciences, 2019, 490, 317-328.	6.9	65
25	Magnetic resonance imaging of myelin using ultrashort Echo time (UTE) pulse sequences: Phantom, specimen, volunteer and multiple sclerosis patient studies. NeuroImage, 2016, 136, 37-44.	4.2	64
26	Ultrashort echo time magnetization transfer (UTEâ€MT) imaging and modeling: magic angle independent biomarkers of tissue properties. NMR in Biomedicine, 2016, 29, 1546-1552.	2.8	63
27	Bone quantitative susceptibility mapping using a chemical species–specific signal model with ultrashort and conventional echo data. Magnetic Resonance in Medicine, 2018, 79, 121-128.	3.0	58
28	Orientational analysis of the Achilles tendon and enthesis using an ultrashort echo time spectroscopic imaging sequence. Magnetic Resonance Imaging, 2010, 28, 178-184.	1.8	55
29	Conventional and Ultrashort Time-to-Echo Magnetic Resonance Imaging of Articular Cartilage, Meniscus, and Intervertebral Disk. Topics in Magnetic Resonance Imaging, 2010, 21, 275-289.	1.2	55
30	Morphology of the Cartilaginous Endplates in Human Intervertebral Disks with Ultrashort Echo Time MR Imaging. Radiology, 2013, 266, 564-574.	7.3	55
31	3D adiabatic T _{1Ï≺/sub> prepared ultrashort echo time cones sequence for whole knee imaging. Magnetic Resonance in Medicine, 2018, 80, 1429-1439.}	3.0	55
32	Short T ₂ imaging using a 3D double adiabatic inversion recovery prepared ultrashort echo time cones (3D DIRâ€UTEâ€Cones) sequence. Magnetic Resonance in Medicine, 2018, 79, 2555-2563.	3.0	55
33	Whole knee joint T ₁ values measured in vivo at 3T by combined 3D ultrashort echo time cones actual flip angle and variable flip angle methods. Magnetic Resonance in Medicine, 2019, 81, 1634-1644.	3.0	52
34	Knee menisci segmentation and relaxometry of 3D ultrashort echo time cones MR imaging using attention Uâ€Net with transfer learning. Magnetic Resonance in Medicine, 2020, 83, 1109-1122.	3.0	51
35	Ultrashort TE imaging with offâ€resonance saturation contrast (UTEâ€OSC). Magnetic Resonance in Medicine, 2009, 62, 527-531.	3.0	50
36	Contrast-enhanced peripheral magnetic resonance angiography using time-resolved vastly undersampled isotropic projection reconstruction. Journal of Magnetic Resonance Imaging, 2004, 20, 894-900.	3.4	47

36

#	Article	IF	CITATIONS
37	Ultrashort echo time magnetization transfer (UTEâ€MT) imaging of cortical bone. NMR in Biomedicine, 2015, 28, 873-880.	2.8	45
38	Whole-Brain Myelin Imaging Using 3D Double-Echo Sliding Inversion Recovery Ultrashort Echo Time (DESIRE UTE) MRI. Radiology, 2020, 294, 362-374.	7.3	45
39	Ultrashort echo time magnetic resonance imaging (UTE-MRI) of cortical bone correlates well with histomorphometric assessment of bone microstructure. Bone, 2019, 123, 8-17.	2.9	44
40	Development of a Comprehensive Osteochondral Allograft MRI Scoring System (OCAMRISS) With Histopathologic, Micro–Computed Tomography, and Biomechanical Validation. Cartilage, 2014, 5, 16-27.	2.7	43
41	Measurement of T1 of the Ultrashort T2* Components in White Matter of the Brain at 3T. PLoS ONE, 2014, 9, e103296.	2.5	43
42	Threeâ€dimensional ultrashort echo time imaging with tricomponent analysis for human cortical bone. Magnetic Resonance in Medicine, 2019, 82, 348-355.	3.0	42
43	MR imaging near metal with undersampled 3D radial UTEâ€MAVRIC sequences. Magnetic Resonance in Medicine, 2013, 69, 27-36.	3.0	40
44	Measurement of bound and pore water T ₁ relaxation times in cortical bone using three-dimensional ultrashort echo time cones sequences. Magnetic Resonance in Medicine, 2017, 77, 2136-2145.	3.0	40
45	Detecting stress injury (fatigue fracture) in fibular cortical bone using quantitative ultrashort echo timeâ€magnetization transfer (UTEâ€MT): An ex vivo study. NMR in Biomedicine, 2018, 31, e3994.	2.8	39
46	Quantitative MRI Musculoskeletal Techniques: An Update. American Journal of Roentgenology, 2019, 213, 524-533.	2.2	39
47	Three-Dimensional Zero Echo Time Magnetic Resonance Imaging Versus 3-Dimensional Computed Tomography for Glenoid Bone Assessment. Arthroscopy - Journal of Arthroscopic and Related Surgery, 2020, 36, 2391-2400.	2.7	39
48	Combined time-resolved and high-spatial-resolution 3D MRA using an extended adaptive acquisition. Journal of Magnetic Resonance Imaging, 2002, 15, 291-301.	3.4	38
49	Evaluation of bound and pore water in cortical bone using ultrashort-TE MRI. NMR in Biomedicine, 2015, 28, 1754-1762.	2.8	38
50	Rotator cuff tendon assessment using magicâ€angle insensitive 3D ultrashort echo time cones magnetization transfer (UTE onesâ€MT) imaging and modeling with histological correlation. Journal of Magnetic Resonance Imaging, 2018, 48, 160-168.	3.4	38
51	Trabecular bone imaging using a 3D adiabatic inversion recovery prepared ultrashort TE Cones sequence at 3T. Magnetic Resonance in Medicine, 2020, 83, 1640-1651.	3.0	38
52	Threeâ€dimensional ultrashort echo time cones <i>T</i> _{1Ï} (3D) Tj ETQq0 0 0 rgBT /Overlock 10 Tf	50 <u>14</u> 2 Td	(UŢĘâ€cone:
53	Optimization of RF excitation to maximize signal and <i>T</i> ₂ contrast of tissues with rapid transverse relaxation. Magnetic Resonance in Medicine, 2010, 64, 481-490.	3.0	36

⁵⁴ Volumetric mapping of bound and pore water as well as collagen protons in cortical bone using 3D ultrashort echo time cones MR imaging techniques. Bone, 2019, 127, 120-128. 2.9

#	Article	IF	CITATIONS
55	Effects of inversion time on inversion recovery prepared ultrashort echo time (IRâ€UTE) imaging of bound and pore water in cortical bone. NMR in Biomedicine, 2015, 28, 70-78.	2.8	35
56	Myelin Imaging in Human Brain Using a Short Repetition Time Adiabatic Inversion Recovery Prepared Ultrashort Echo Time (STAIR-UTE) MRI Sequence in Multiple Sclerosis. Radiology, 2020, 297, 392-404.	7.3	35
57	Quantitative twoâ€dimensional ultrashort echo time magnetization transfer (2D UTEâ€MT) imaging of cortical bone. Magnetic Resonance in Medicine, 2018, 79, 1941-1949.	3.0	34
58	Collagen proton fraction from ultrashort echo time magnetization transfer (UTEâ€MT) MRI modelling correlates significantly with cortical bone porosity measured with microâ€computed tomography (μCT). NMR in Biomedicine, 2019, 32, e4045.	2.8	34
59	Significant correlations between human cortical bone mineral density and quantitative susceptibility mapping (QSM) obtained with 3D Cones ultrashort echo time magnetic resonance imaging (UTE-MRI). Magnetic Resonance Imaging, 2019, 62, 104-110.	1.8	34
60	Fast quantitative 3D ultrashort echo time MRI of cortical bone using extended cones sampling. Magnetic Resonance in Medicine, 2019, 82, 225-236.	3.0	34
61	Magnetic resonance imaging (MRI) studies of knee joint under mechanical loading: Review. Magnetic Resonance Imaging, 2020, 65, 27-36.	1.8	34
62	Fast volumetric imaging of bound and pore water in cortical bone using threeâ€dimensional ultrashortâ€TE (UTE) and inversion recovery UTE sequences. NMR in Biomedicine, 2016, 29, 1373-1380.	2.8	33
63	Three-dimensional ultrashort echo time cones (3D UTE-Cones) magnetic resonance imaging of entheses and tendons. Magnetic Resonance Imaging, 2018, 49, 4-9.	1.8	33
64	Correlations of cortical bone microstructural and mechanical properties with water proton fractions obtained from ultrashort echo time (UTE) MRI tricomponent T2* model. NMR in Biomedicine, 2020, 33, e4233.	2.8	33
65	Highâ€resolution timeâ€resolved contrastâ€enhanced MR abdominal and pulmonary angiography using a spiralâ€TRICKS sequence. Magnetic Resonance in Medicine, 2007, 58, 631-635.	3.0	32
66	Single- and Bi-component T2* analysis of tendon before and during tensile loading, using UTE sequences. Journal of Magnetic Resonance Imaging, 2015, 42, 114-120.	3.4	32
67	Assessing cortical bone mechanical properties using collagen proton fraction from ultrashort echo time magnetization transfer (UTE-MT) MRI modeling. Bone Reports, 2019, 11, 100220.	0.4	32
68	Fat suppression for ultrashort echo time imaging using a singleâ€point Dixon method. NMR in Biomedicine, 2019, 32, e4069.	2.8	32
69	Quantitative Ultrashort Echo Time (UTE) Magnetic Resonance Imaging of Bone: An Update. Frontiers in Endocrinology, 2020, 11, 567417.	3.5	31
70	Convincing evidence for magic angle lessâ€sensitive quantitative T _{1Ï} imaging of articular cartilage using the 3D ultrashort echo time cones adiabatic T _{1Ï} Â(3D UTE) Tj ETQq0 0 0 rgBT /Overlo	ock3100 Tf	50 3 B7 Td (
	Ultrashort Echo Time Magnetic Resonance Imaging Techniques: Met and Unmet Needs in	3.4	30

/1	Musculoskeletal Imaging. Journal of Magnetic Resonance Imaging, 2022, 55, 1597-1612.	0.4	30
72	Meniscal Calcifications: Morphologic and Quantitative Evaluation by using 2D Inversion-Recovery Ultrashort Echo Time and 3D Ultrashort Echo Time 3.0-T MR Imaging Techniques—Feasibility Study. Radiology, 2012, 264, 260-268.	7.3	29

#	Article	IF	CITATIONS
73	Incorporating prior knowledge via volumetric deep residual network to optimize the reconstruction of sparsely sampled MRI. Magnetic Resonance Imaging, 2020, 66, 93-103.	1.8	29
74	Can ultrashort-TE (UTE) MRI sequences on a 3-T clinical scanner detect signal directly from collagen protons: freeze-dry and D ₂ O exchange studies of cortical bone and Achilles tendon specimens. NMR in Biomedicine, 2016, 29, 912-917.	2.8	28
75	Effects of achilles tendon immersion in saline and perfluorochemicals on T2 and T2*. Journal of Magnetic Resonance Imaging, 2014, 40, 496-500.	3.4	27
76	Quantitative 3D ultrashort time-to-echo (UTE) MRI and micro-CT (μCT) evaluation of the temporomandibular joint (TMJ) condylar morphology. Skeletal Radiology, 2014, 43, 19-25.	2.0	27
77	Yet more evidence that myelin protons can be directly imaged with UTE sequences on a clinical 3 <scp>T</scp> scanner: Bicomponent analysis of native and deuterated ovine brain specimens. Magnetic Resonance in Medicine, 2018, 80, 538-547.	3.0	27
78	Imaging of the region of the osteochondral junction (OCJ) using a 3D adiabatic inversion recovery prepared ultrashort echo time cones (3D IRâ€UTEâ€cones) sequence at 3ÂT. NMR in Biomedicine, 2019, 32, e4080.	2.8	27
79	Age-related decrease in collagen proton fraction in tibial tendons estimated by magnetization transfer modeling of ultrashort echo time magnetic resonance imaging (UTE-MRI). Scientific Reports, 2019, 9, 17974.	3.3	27
80	Ultrashort TE <i>T</i> ₁ ï•magic angle imaging. Magnetic Resonance in Medicine, 2013, 69, 682-687.	3.0	26
81	Effects of repetitive freeze–thawing cycles on T2 and T2* of the Achilles tendon. European Journal of Radiology, 2014, 83, 349-353.	2.6	26
82	Magnetic resonance imaging assessed cortical porosity is highly correlated with $\hat{1}$ /4CT porosity. Bone, 2014, 66, 56-61.	2.9	26
83	Simultaneous quantitative susceptibility mapping (QSM) and for high iron concentration quantification with 3D ultrashort echo time sequences: An echo dependence study. Magnetic Resonance in Medicine, 2018, 79, 2315-2322.	3.0	26
84	Direct imaging and quantification of carotid plaque calcification. Magnetic Resonance in Medicine, 2011, 65, 1013-1020.	3.0	25
85	Evaluation of normal cadaveric Achilles tendon and enthesis with ultrashort echo time (UTE) magnetic resonance imaging and indentation testing. NMR in Biomedicine, 2019, 32, e4034.	2.8	25
86	<i>k</i> â€space waterâ€fat decomposition with T ₂ * estimation and multifrequency fat spectrum modeling for ultrashort echo time imaging. Journal of Magnetic Resonance Imaging, 2010, 31, 1027-1034.	3.4	24
87	Feasibility of using an inversion-recovery ultrashort echo time (UTE) sequence for quantification of glenoid bone loss. Skeletal Radiology, 2018, 47, 973-980.	2.0	24
88	Fat suppression for ultrashort echo time imaging using a novel softâ€hard composite radiofrequency pulse. Magnetic Resonance in Medicine, 2019, 82, 2178-2187.	3.0	24
89	True phase quantitative susceptibility mapping using continuous singleâ€point imaging: a feasibility study. Magnetic Resonance in Medicine, 2019, 81, 1907-1914.	3.0	24
90	Qualitative and Quantitative Ultrashort Echo Time Imaging of Musculoskeletal Tissues. Seminars in Musculoskeletal Radiology, 2015, 19, 375-386.	0.7	23

#	Article	IF	CITATIONS
91	Dynamic MR venography: An intrinsic benefit of time-resolved MR angiography. Journal of Magnetic Resonance Imaging, 2006, 24, 922-927.	3.4	22
92	Comparison of T1rho Measurements in Agarose Phantoms and Human Patellar Cartilage Using 2D Multislice Spiral and 3D Magnetization Prepared Partitioned k-Space Spoiled Gradient-Echo Snapshot Techniques at 3 T. American Journal of Roentgenology, 2011, 196, W174-W179.	2.2	21
93	Advanced Hemophilic Arthropathy: Sensitivity of Soft Tissue Discrimination With Musculoskeletal Ultrasound. Journal of Ultrasound in Medicine, 2018, 37, 1945-1956.	1.7	21
94	Advanced magnetic resonance imaging of cartilage components in haemophilic joints reveals that cartilage hemosiderin correlates with joint deterioration. Haemophilia, 2019, 25, 851-858.	2.1	20
95	In vivo assessment of extracellular pH of joint tissues using acidoCEST-UTE MRI. Quantitative Imaging in Medicine and Surgery, 2019, 9, 1664-1673.	2.0	20
96	Ultrashort echo time quantitative susceptibility mapping (UTEâ€QSM) for detection of hemosiderin deposition in hemophilic arthropathy: A feasibility study. Magnetic Resonance in Medicine, 2020, 84, 3246-3255.	3.0	20
97	Interleaved variable density sampling with a constrained parallel imaging reconstruction for dynamic contrastâ€enhanced MR angiography. Magnetic Resonance in Medicine, 2011, 66, 428-436.	3.0	19
98	MR Parametric Mapping as a Biomarker of Early Joint Degeneration. Sports Health, 2016, 8, 405-411.	2.7	19
99	Inversion recovery ultrashort echo time imaging of ultrashort <i>T</i> ₂ tissue components in ovine brain at 3ÂT: a sequential D ₂ O exchange study. NMR in Biomedicine, 2017, 30, e3767.	2.8	19
100	Three-dimensional adiabatic inversion recovery prepared ultrashort echo time cones (3D IR-UTE-Cones) imaging of cortical bone in the hip. Magnetic Resonance Imaging, 2017, 44, 60-64.	1.8	19
101	Ultrashort Echo Time Quantitative Susceptibility Mapping (UTE-QSM) of Highly Concentrated Magnetic Nanoparticles: A Comparison Study about Different Sampling Strategies. Molecules, 2019, 24, 1143.	3.8	19
102	An Update in Qualitative Imaging of Bone Using Ultrashort Echo Time Magnetic Resonance. Frontiers in Endocrinology, 2020, 11, 555756.	3.5	19
103	Magic angle effect on adiabatic T _{1Ï} imaging of the Achilles tendon using 3D ultrashort echo time cones trajectory. NMR in Biomedicine, 2020, 33, e4322.	2.8	18
104	Contrastâ€enhanced MR angiography using time resolved interleaved projection sampling with threeâ€dimensional cartesian phase and slice encoding (TRIPPS). Magnetic Resonance in Medicine, 2009, 61, 918-924.	3.0	17
105	Imaging and quantification of ironâ€oxide nanoparticles (IONP) using MPâ€RAGE and UTE based sequences. Magnetic Resonance in Medicine, 2017, 78, 226-232.	3.0	17
106	Quantitative threeâ€dimensional ultrashort echo time cones imaging of the knee joint with motion correction. NMR in Biomedicine, 2020, 33, e4214.	2.8	17
107	Magnetic resonance imaging of the shoulder. Polish Journal of Radiology, 2020, 85, 420-439.	0.9	17
108	Ultrashort echo time biâ€component analysis of cortical bone—a field dependence study. Magnetic Resonance in Medicine. 2014. 71. 1075-1081.	3.0	16

#	Article	IF	CITATIONS
109	Inversion recovery ultrashort echo time magnetic resonance imaging: A method for simultaneous direct detection of myelin and high signal demonstration of iron deposition in the brain – A feasibility study. Magnetic Resonance Imaging, 2017, 38, 87-94.	1.8	16
110	Ultrashort echo time (UTE) magnetic resonance imaging of myelin: technical developments and challenges. Quantitative Imaging in Medicine and Surgery, 2020, 10, 1186-1203.	2.0	16
111	Quantitative ultrashort echo time magnetization transfer (UTE-MT) for diagnosis of early cartilage degeneration: comparison with UTE-T2* and T2 mapping. Quantitative Imaging in Medicine and Surgery, 2020, 10, 171-183.	2.0	16
112	Ultrashort echo time T2 â^— values decrease in tendons with application of static tensile loads. Journal of Biomechanics, 2017, 61, 160-167.	2.1	15
113	Inversion recovery UTE based volumetric myelin imaging in human brain using interleaved hybrid encoding. Magnetic Resonance in Medicine, 2020, 83, 950-961.	3.0	15
114	Water proton density in human cortical bone obtained from ultrashort echo time (UTE) MRI predicts bone microstructural properties. Magnetic Resonance Imaging, 2020, 67, 85-89.	1.8	15
115	Accelerating quantitative MR imaging with the incorporation of B1 compensation using deep learning. Magnetic Resonance Imaging, 2020, 72, 78-86.	1.8	15
116	Volumetric imaging of myelin in vivo using 3D inversion recoveryâ€prepared ultrashort echo time cones magnetic resonance imaging. NMR in Biomedicine, 2020, 33, e4326.	2.8	15
117	MRI chemical shift artifact produced by center-out radial sampling of k-space: a potential pitfall in clinical diagnosis. Quantitative Imaging in Medicine and Surgery, 2021, 11, 3677-3683.	2.0	15
118	Noise reduction in MR angiography with nonlinear anisotropic filtering. Journal of Magnetic Resonance Imaging, 2004, 19, 632-639.	3.4	14
119	Quantitative Ultrasound and B-Mode Image Texture Features Correlate with Collagen and Myelin Content in Human Ulnar Nerve Fascicles. Ultrasound in Medicine and Biology, 2019, 45, 1830-1840.	1.5	14
120	Single- and Bicomponent Analyses of T2 <mml:math <br="" xmlns:mml="http://www.w3.org/1998/Math/MathML">id="M1"><mml:mrow><mml:mo>âŽ</mml:mo></mml:mrow></mml:math> Relaxation in Knee Tendon and Ligament by Using 3D Ultrashort Echo Time Cones (UTE Cones) Magnetic Resonance Imaging. BioMed Research International, 2019, 2019, 1-9.	1.9	14
121	Assessment of mechanical properties of articular cartilage with quantitative three-dimensional ultrashort echo time (UTE) cones magnetic resonance imaging. Journal of Biomechanics, 2020, 113, 110085.	2.1	14
122	Inversion recovery zero echo time (IR-ZTE) imaging for direct myelin detection in human brain: a feasibility study. Quantitative Imaging in Medicine and Surgery, 2020, 10, 895-906.	2.0	14
123	Automated cartilage segmentation and quantification using 3D ultrashort echo time (UTE) cones MR imaging with deep convolutional neural networks. European Radiology, 2021, 31, 7653-7663.	4.5	14
124	Magnetic resonance imaging of the temporomandibular joint disc: feasibility of novel quantitative magnetic resonance evaluation using histologic and biomechanical reference standards. Journal of Orofacial Pain, 2011, 25, 345-53.	1.7	14
125	Time-resolved contrast-enhanced carotid imaging using undersampled projection reconstruction acquisition. Journal of Magnetic Resonance Imaging, 2007, 25, 1093-1099.	3.4	13
126	Thickness of the Meniscal Lamellar Layer: Correlation with Indentation Stiffness and Comparison of Normal and Abnormally Thick Layers by Using Multiparametric Ultrashort Echo Time MR Imaging. Radiology, 2016, 280, 161-168.	7.3	13

#	Article	IF	CITATIONS
127	MR morphology of triangular fibrocartilage complex: correlation with quantitative MR and biomechanical properties. Skeletal Radiology, 2016, 45, 447-454.	2.0	13
128	MR Arthrogram Features That Can Be Used to Distinguish Between True Inferior Glenohumeral Ligament Complex Tears and latrogenic Extravasation. American Journal of Roentgenology, 2019, 212, 411-417.	2.2	13
129	Quantitative bi-component T2* analysis of histologically normal Achilles tendons. Muscles, Ligaments and Tendons Journal, 2015, 5, 58-62.	0.3	13
130	AcidoCEST-UTE MRI Reveals an Acidic Microenvironment in Knee Osteoarthritis. International Journal of Molecular Sciences, 2022, 23, 4466.	4.1	13
131	Direct magnitude and phase imaging of myelin using ultrashort echo time (UTE) pulse sequences: A feasibility study. Magnetic Resonance Imaging, 2017, 39, 194-199.	1.8	12
132	Rotator Cuff Tendon Assessment in Symptomatic and Control Groups Using Quantitative MRI. Journal of Magnetic Resonance Imaging, 2020, 52, 864-872.	3.4	12
133	Ultrashort echo time Cones double echo steady state (UTEâ€Conesâ€DESS) for rapid morphological imaging of short T ₂ tissues. Magnetic Resonance in Medicine, 2021, 86, 881-892.	3.0	12
134	Quantitative <scp>3D</scp> Ultrashort Echo Time Magnetization Transfer Imaging for Evaluation of Knee Cartilage Degeneration In Vivo. Journal of Magnetic Resonance Imaging, 2021, 54, 1294-1302.	3.4	12
135	Improved volumetric myelin imaging in human brain using 3D dual echo inversion recoveryâ€prepared UTE with complex echo subtraction. Magnetic Resonance in Medicine, 2020, 83, 1168-1177.	3.0	11
136	Pulse sequences as tissue property filters (TP-filters): a way of understanding the signal, contrast and weighting of magnetic resonance images. Quantitative Imaging in Medicine and Surgery, 2020, 10, 1080-1120.	2.0	11
137	Ultrashort Echo Time MRI (UTE-MRI) Quantifications of Cortical Bone Varied Significantly at Body Temperature Compared with Room Temperature. Investigative Magnetic Resonance Imaging, 2019, 23, 202.	0.4	11
138	Mineralization in calcified plaque is like that of cortical bone—Further evidence from ultrashort echo time (UTE) magnetic resonance imaging of carotid plaque calcification and cortical bone. Medical Physics, 2013, 40, 102301.	3.0	10
139	Effects of fat saturation on short T2 quantification. Magnetic Resonance Imaging, 2017, 43, 6-9.	1.8	10
140	Assessing the Performance of Morphologic and Echogenic Features in Median Nerve Ultrasound for Carpal Tunnel Syndrome Diagnosis. Journal of Ultrasound in Medicine, 2020, 39, 1165-1174.	1.7	10
141	Brain ultrashort T2 component imaging using a short TR adiabatic inversion recovery prepared dual-echo ultrashort TE sequence with complex echo subtraction (STAIR-dUTE-ES). Journal of Magnetic Resonance, 2021, 323, 106898.	2.1	10
142	Correlation between the elastic modulus of anterior cruciate ligament (ACL) and quantitative ultrashort echo time (UTE) magnetic resonance imaging. Journal of Orthopaedic Research, 2022, 40, 2330-2339.	2.3	10
143	High-resolution morphologic and ultrashort time-to-echo quantitative magnetic resonance imaging of the temporomandibular joint. Skeletal Radiology, 2016, 45, 383-391.	2.0	9
144	Theoretical analysis and optimization of ultrashort echo time (UTE) imaging contrast with off-resonance saturation. Magnetic Resonance Imaging, 2018, 50, 12-16.	1.8	9

#	Article	IF	CITATIONS
145	T ₁ measurement of bound water in cortical bone using 3D adiabatic inversion recovery ultrashort echo time (3D IRâ€UTE) Cones imaging. Magnetic Resonance in Medicine, 2020, 84, 634-645.	3.0	9
146	To measure T1 of short T2 species using an inversion recovery prepared three-dimensional ultrashort echo time (3D IR-UTE) method: A phantom study. Journal of Magnetic Resonance, 2020, 314, 106725.	2.1	9
147	Quantitative Magnetic Resonance Imaging of Cortical and Trabecular Bone. Seminars in Musculoskeletal Radiology, 2020, 24, 386-401.	0.7	9
148	Ultrashort TE MR imaging of bovine cortical bone: The effect of water loss on the <i>T</i> ₁ and <i>T</i> ₂ * relaxation times. Magnetic Resonance in Medicine, 2011, 66, 476-482.	3.0	8
149	Evaluation of cortical bone perfusion using dynamic contrast enhanced ultrashort echo time imaging: a feasibility study. Quantitative Imaging in Medicine and Surgery, 2019, 9, 1383-1393.	2.0	8
150	Assessment of an in vitro model of rotator cuff degeneration using quantitative magnetic resonance and ultrasound imaging with biochemical and histological correlation. European Journal of Radiology, 2019, 121, 108706.	2.6	8
151	AcidoCEST-UTE MRI for the Assessment of Extracellular pH of Joint Tissues at 3 T. Investigative Radiology, 2019, 54, 565-571.	6.2	8
152	Detecting Articular Cartilage and Meniscus Deformation Effects Using Magnetization Transfer Ultrashort Echo Time (MT-UTE) Modeling during Mechanical Load Application: Ex Vivo Feasibility Study. Cartilage, 2020, , 194760352097677.	2.7	8
153	Ultrashort TE spectroscopic imaging (UTESI) using complex highlyâ€constrained backprojection with local reconstruction (HYPR LR). Magnetic Resonance in Medicine, 2009, 62, 127-134.	3.0	7
154	Optimizing MR signal contrast of the temporomandibular joint disk. Journal of Magnetic Resonance Imaging, 2011, 34, 1458-1464.	3.4	7
155	Nonoperative Management of a Severe Proximal Rectus Femoris Musculotendinous Injury in a Recreational Athlete: A Case Report. PM and R, 2018, 10, 1417-1421.	1.6	7
156	Rapid single scan ramped hybridâ€encoding for bicomponent T2* mapping in a human knee joint: A feasibility study. NMR in Biomedicine, 2020, 33, e4391.	2.8	7
157	Use of Multiplied, Added, Subtracted and/or FiTted Inversion Recovery (MASTIR) pulse sequences. Quantitative Imaging in Medicine and Surgery, 2020, 10, 1334-1369.	2.0	7
158	Comprehensive assessment of in vivo lumbar spine intervertebral discs using a 3D adiabatic T1ϕprepared ultrashort echo time (UTE-Adiab-T1Ï) pulse sequence. Quantitative Imaging in Medicine and Surgery, 2022, 12, 269-280.	2.0	7
159	A Useful Combination of Quantitative Ultrashort Echo Time MR Imaging and a Probing Device for Biomechanical Evaluation of Articular Cartilage. Biosensors, 2021, 11, 52.	4.7	7
160	Time-resolved undersampled projection reconstruction magnetic resonance imaging of the peripheral vessels using multi-echo acquisition. Magnetic Resonance in Medicine, 2005, 53, 730-734.	3.0	6
161	Radiofrequency pulses for simultaneous short <i>T</i> ₂ excitation and long <i>T</i> ₂ suppression. Magnetic Resonance in Medicine, 2011, 65, 531-537.	3.0	6
162	The effect of excitation and preparation pulses on nonslice selective 2D UTE bicomponent analysis of bound and free water in cortical bone at 3T. Medical Physics, 2014, 41, 022306.	3.0	6

#	Article	IF	CITATIONS
163	Susceptibility-Based Neuroimaging: Standard Methods, Clinical Applications, and Future Directions. Current Radiology Reports, 2017, 5, 1.	1.4	6
164	Pectoralis major tendon and enthesis: anatomic, magnetic resonance imaging, ultrasonographic, and histologicÂinvestigation. Journal of Shoulder and Elbow Surgery, 2020, 29, 1590-1598.	2.6	6
165	High contrast cartilaginous endplate imaging using a 3D adiabatic inversionâ€recoveryâ€prepared fatâ€saturated ultrashort echo time (3D IRâ€FSâ€UTE) sequence. NMR in Biomedicine, 2021, 34, e4579.	2.8	6
166	Feasibility of an Inversion Recovery-Prepared Fat-Saturated Zero Echo Time Sequence for High Contrast Imaging of the Osteochondral Junction. Frontiers in Endocrinology, 2021, 12, 777080.	3.5	6
167	Ultrashort Echo Time T1ï•Is Sensitive to Enzymatic Degeneration of Human Menisci. Journal of Computer Assisted Tomography, 2015, 39, 637-642.	0.9	5
168	High-Resolution Qualitative and Quantitative Magnetic Resonance Evaluation of the Glenoid Labrum. Journal of Computer Assisted Tomography, 2015, 39, 936-944.	0.9	5
169	New options for increasing the sensitivity, specificity and scope of synergistic contrast magnetic resonance imaging (scMRI) using Multiplied, Added, Subtracted and/or FiTted (MASTIR) pulse sequences. Quantitative Imaging in Medicine and Surgery, 2020, 10, 2030-2065.	2.0	5
170	Fast quantitative threeâ€dimensional ultrashort echo time (UTE) Cones magnetic resonance imaging of major tissues in the knee joint using extended sprial sampling. NMR in Biomedicine, 2020, 33, e4376.	2.8	5
171	Ultrashort echo time adiabatic T1Ï•(UTE-Adiab-T1Ï) is sensitive to human cadaveric knee joint deformation induced by mechanical loading and unloading. Magnetic Resonance Imaging, 2021, 80, 98-105.	1.8	5
172	MRI-based mechanical competence assessment of bone using micro finite element analysis (micro-FEA): Review. Magnetic Resonance Imaging, 2022, 88, 9-19.	1.8	5
173	Quantitative assessment of articular cartilage degeneration using 3D ultrashort echo time cones adiabatic T1ï•(3D UTE-Cones-AdiabT1ï) imaging. European Radiology, 2022, 32, 6178-6186.	4.5	5
174	Lower Macromolecular Content in Tendons of Female Patients with Osteoporosis versus Patients with Osteopenia Detected by Ultrashort Echo Time (UTE) MRI. Diagnostics, 2022, 12, 1061.	2.6	5
175	Whole-body MR angiography using variable density sampling and dual-injection bolus-chase acquisition. Magnetic Resonance Imaging, 2008, 26, 181-187.	1.8	4
176	Automated vessel segmentation using cross-correlation and pooled covariance matrix analysis. Magnetic Resonance Imaging, 2011, 29, 391-400.	1.8	4
177	Offâ€resonance saturation ratio obtained with ultrashort echo timeâ€magnetization transfer techniques is sensitive to changes in static tensile loading of tendons and degeneration. Journal of Magnetic Resonance Imaging, 2015, 42, 1064-1071.	3.4	4
178	Feasibility of quantitative ultrashort echo time (UTE)â€based methods for MRI of peripheral nerve. NMR in Biomedicine, 2018, 31, e3948.	2.8	4
179	Quantitative magnetic resonance imaging of meniscal pathology ex vivo. Skeletal Radiology, 2021, 50, 2405-2414.	2.0	4
180	Hippocampal and thalamic neuronal metabolism in a putative rat model of schizophrenia. Neural Regeneration Research, 2013, 8, 2415-23.	3.0	4

#	Article	IF	CITATIONS
181	Evaluation of enzymatic proteoglycan loss and collagen degradation in human articular cartilage using ultrashort echo timeâ€based biomarkers: A feasibility study. NMR in Biomedicine, 2022, 35, e4664.	2.8	4
182	Contrast-enhanced MR angiography with frequency-dependent mask subtraction. Magnetic Resonance Imaging, 2009, 27, 1326-1332.	1.8	3
183	Magnetic resonance ultrashort echo time spin-echo imaging of the deepest layers of articular cartilage. Science China Life Sciences, 2013, 56, 672-674.	4.9	3
184	Brain Atrophy Is a Better Biomarker than Susceptibility for Evaluating Clinical Severity in Wilson Disease. Radiology, 2021, 299, 673-674.	7.3	3
185	Evaluation of cartilage degeneration using multiparametric quantitative ultrashort echo time-based MRI: an ex vivo study. Quantitative Imaging in Medicine and Surgery, 2022, 12, 1738-1749.	2.0	3
186	Maximizing MR signal for 2D UTE slice selection in the presence of rapid transverse relaxation. Magnetic Resonance Imaging, 2014, 32, 1006-1011.	1.8	2
187	Signal and contrast effects due to T2 decay during k-space readout of UTE (ultrashort TE) sequences. Magnetic Resonance Imaging, 2014, 32, 259-269.	1.8	2
188	Multimodal imaging assessment and histologic correlation of the female rat pelvic floor muscles' anatomy. Journal of Anatomy, 2019, 234, 543-550.	1.5	2
189	Detection of gadolinium deposition in cortical bone with ultrashort echo time T1 mapping: an ex vivo study in a rabbit model. European Radiology, 2021, 31, 1569-1577.	4.5	1
190	Optimizing Diffusion-weighted MRI of Peripheral Nerves. Radiology, 2022, 302, 162-163.	7.3	1
191	The Resistance Force of the Anterior Cruciate Ligament during Pull Probing Is Related to the Mechanical Property. Bioengineering, 2022, 9, 4.	3.5	1
192	Editorial for "Change in Susceptibility Values in Knee Cartilage After Marathon Running Measured Using Quantitative Susceptibility Mapping― Journal of Magnetic Resonance Imaging, 2021, 54, 1594-1595.	3.4	0
193	Editorial for "Association Between <scp>T2</scp> * Relaxation Times Derived from Ultrashort Echo Time <scp>MRI</scp> and Symptoms During Exercise Therapy for Patellar Tendinopathy: A Large Prospective Study― Journal of Magnetic Resonance Imaging, 2021, 54, 1606-1607.	3.4	0